Clustering and response functions of light nuclei in explicitly correlated Gaussians (ECG)

Y. Suzuki (Niigata, Riken)

Motivation: Unified description of nuclear states with different character
e.g. particle-hole excitation, spatially localized clustering
Solving problems relevant to continuum
e.g. resonance, response functions

We show our recent works for light nuclei performed in few-body approach:

Spectrum of ^4He, E1 and spin-dipole responses of ^4He
(4-body calculation with realistic force)
E1 response of a halo nucleus ^6He
(6-body calculation with effective central force)
Coexistence of shell-model and clustering states in ^{16}O
(^{12}C+n+n+p+p 5-body calculation)

ECG describes correlations and asymptotics properly
Complex scaling method(CSM) converts continuum problems to those of L^2 basis

Nordita workshop 'Computational challenges in nuclear and many-body physics'
Sept. 15 – Oct. 10, 2014 Stockholm

ECG basis

Spherical Gaussian: $\exp\left(-\sum_{i<j}\frac{1}{2b_{ij}^2}(\boldsymbol{r}_i-\boldsymbol{r}_j)^2\right) \rightarrow \exp\left(-\frac{1}{2}\tilde{\boldsymbol{x}}A\boldsymbol{x}\right)$

N-particle system: $N-1$ relative coordinates $\tilde{\boldsymbol{x}} = (\boldsymbol{x}_1, \boldsymbol{x}_2, \ldots, \boldsymbol{x}_{N-1})$ $\quad \boldsymbol{x} = \begin{pmatrix} \boldsymbol{x}_1 \\ \boldsymbol{x}_2 \\ \vdots \\ \boldsymbol{x}_{N-1} \end{pmatrix}$

$$\tilde{\boldsymbol{x}}A\boldsymbol{x} = \sum_{i,j} A_{ij}\boldsymbol{x}_i \cdot \boldsymbol{x}_j \qquad A_{ij} = A_{ji}$$

Non-spherical motion: Global vector $\tilde{u}\boldsymbol{x} = u_1\boldsymbol{x}_1 + u_2\boldsymbol{x}_2 + \ldots + u_{N-1}\boldsymbol{x}_{N-1}$
(angular part)

$$[\mathcal{Y}_{L_1}(\tilde{u}\boldsymbol{x}) \times \mathcal{Y}_{L_2}(\tilde{v}\boldsymbol{x})]_{LM} \qquad \mathcal{Y}_\ell(\boldsymbol{r}) = r^\ell Y_\ell(\hat{\boldsymbol{r}})$$

General form:

$$\Phi_\alpha = \mathcal{A}\left\{\exp\left(-\frac{1}{2}\tilde{\boldsymbol{x}}A\boldsymbol{x}\right)\left[\left[\mathcal{Y}_{L_1}(\tilde{u}\boldsymbol{x}) \times \mathcal{Y}_{L_2}(\tilde{v}\boldsymbol{x})\right]_L \times \chi^{(\mathrm{Spin})}_{S_{12}S_{123}\ldots S}\right]_{JM}\eta^{(\mathrm{Isopin})}_{T_{12}T_{123}\ldots TM_T}\right\}$$

Variational parameters: Continuous A, u, v Discrete $L_1, L_2, L, S, \ldots$

$$\pi = +: \ L\text{=even } (L_1{=}L,\ L_2{=}0), \ \ L\text{=odd } (L_1{=}L,\ L_2{=}1)$$

Trial function $\quad \Psi = \sum_\alpha C_\alpha \Phi_\alpha$

$$H = \sum_{i=1}^{N} T_i - T_{\mathrm{c.m.}} + \sum_{i<j} v_{ij} + \sum_{i<j<k} v_{ijk}$$

Main features

Fully microscopic
No spurious c.m. motion
Adaptable to arbitrary N-particle system
Analytic evaluation of matrix elements
Invariance under a linear coordinate transformation

$$\boldsymbol{y} = T\boldsymbol{x}$$

$$\exp\left(-\widetilde{\boldsymbol{y}}B\boldsymbol{y}\right)\mathcal{Y}_{LM}(\widetilde{v}\boldsymbol{y}) = \exp\left(-\widetilde{\boldsymbol{x}}A\boldsymbol{x}\right)\mathcal{Y}_{LM}(\widetilde{u}\boldsymbol{x})$$

$$A = \tilde{T}BT, \;\; u = \tilde{T}v$$

s.p. motion

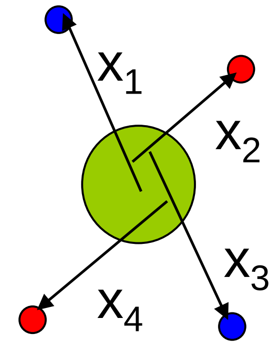

ECG is flexible in describing various correlations and asymptotics in a single scheme

clustering

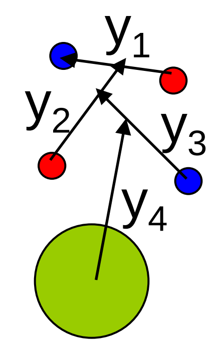

Recent applications of ECG: J. Mitroy et al., RMP 85 (2013)

Basis selection

Stochastic variational method (SVM)

K.Varga, Y.S., PRC 52 (1995)
Y.S., K. Varga, Lecture notes in physics 54 (Springer, 1998)

Four-nucleon system: ^{4}He

Kamada et al., PRC64 (2001)

Simultaneous description of both 0_1^+ and 0_2^+ states that have quite different structure

AV8' + 3NF

Central, Tensor, LS
Strong short-range repulsion

Energy convergence

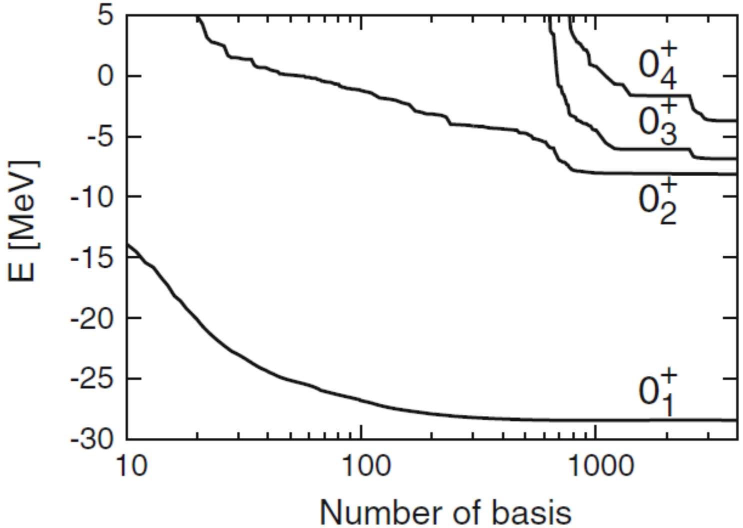

The first 1000 bases: $(0 < b_{ij} < 16$ fm)
Beyond 1000: 3N+N type bases

One-body density

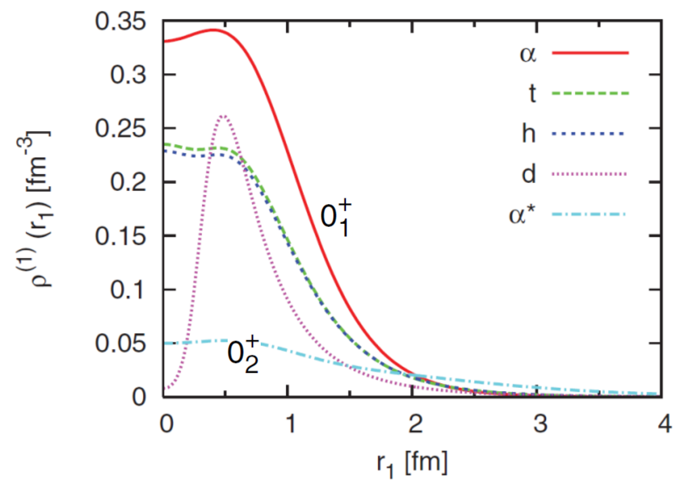

^{3}H+p spectroscopic amplitude

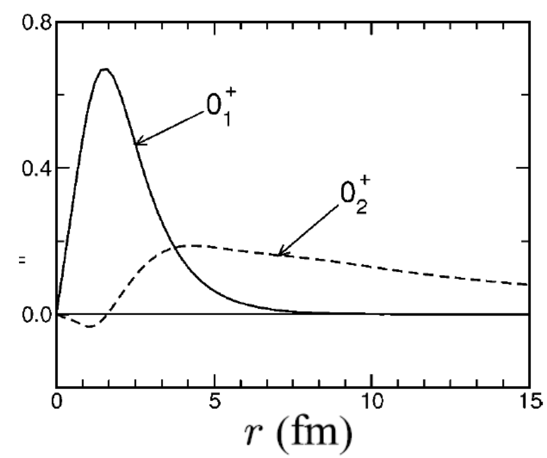

Hiyama,Gibson,Kamimura,PRC70 (2004)

Spectrum of ^{4}He

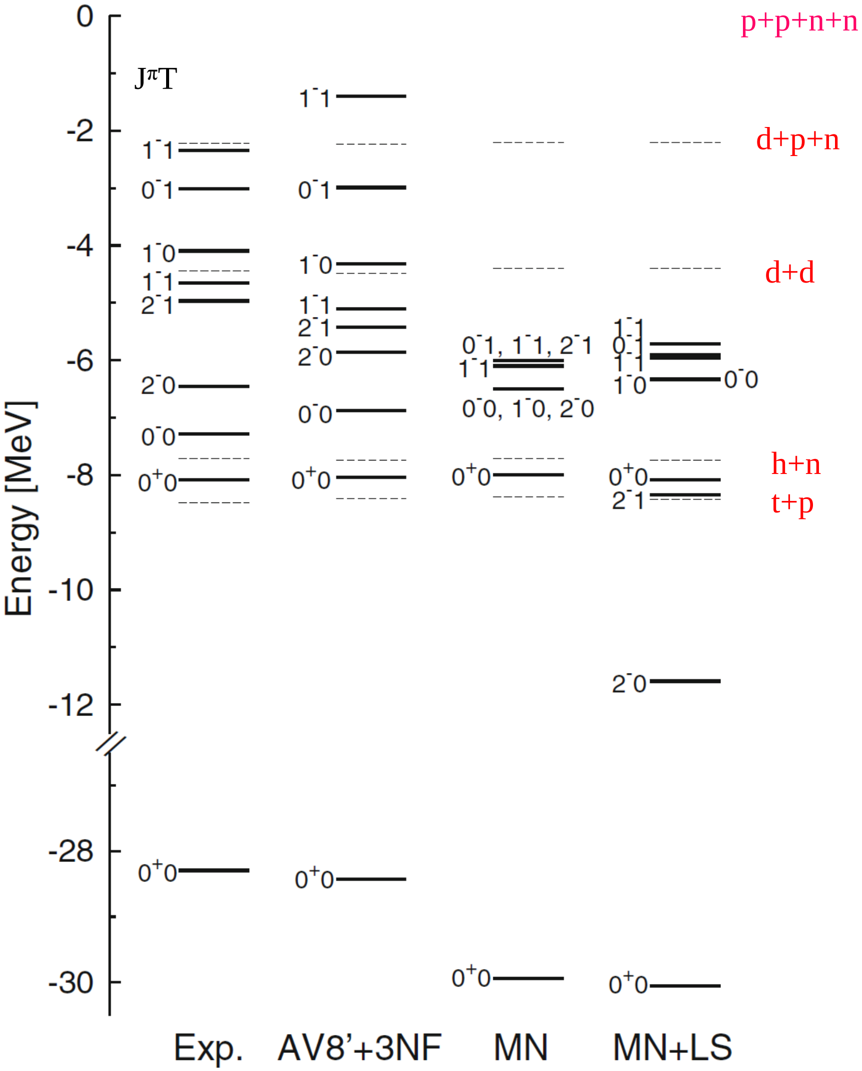

Realistic force well reproduces spectrum

Level sequence: T=0: 0^-, 2^-, 1^-

T=1: 2^-, 1^-, 0^-, 1^-

Three lowest negative-parity states have 3N+N cluster structure with P-wave relative motion:

Parity-inverted partner of the 0_2^+ state

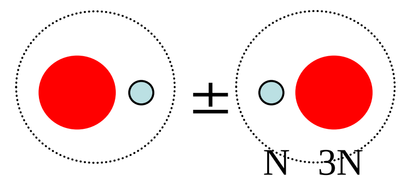

Distribution of HO quanta Q

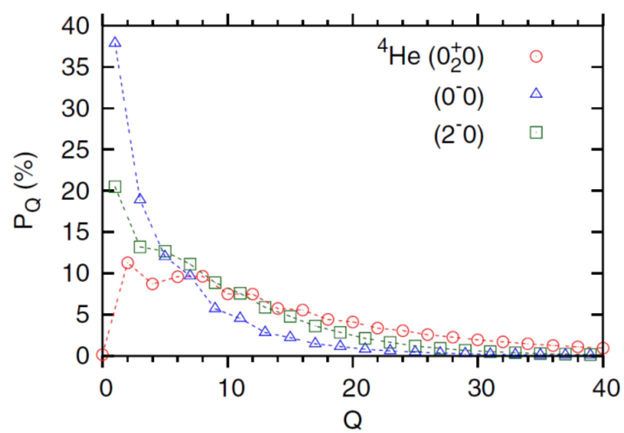

1p-1h is largest for 0^- and 2^-

Large P_Q for high Q

Most of the negative parity states are broad resonances $\longrightarrow$ response function

CSM

Response (strength) function

$$S(E) = \mathcal{S}_{\mu f} |\langle \Psi_f | \mathcal{M}_{1\mu} | \Psi_0 \rangle|^2 \delta(E_f - E_0 - E)$$

$\mathcal{M}_{1\mu}$: E1 operator

$$= -\frac{1}{\pi} \mathrm{Im} \sum_{\mu} \langle \Psi_0 | \mathcal{M}^{\dagger}_{1\mu} \frac{1}{E - H + E_0 + i\epsilon} \mathcal{M}_{1\mu} | \Psi_0 \rangle$$

many-body resolvent

Continuum discretization with CSM

Moiseyev, Phys. Rep. 302 (1998)

$$U(\theta): \quad \boldsymbol{r}_j \to \boldsymbol{r}_j e^{i\theta}, \quad \boldsymbol{p}_j \to \boldsymbol{p}_j e^{-i\theta}$$

$$e^{i\boldsymbol{k}\cdot\boldsymbol{r}} \longrightarrow e^{\boldsymbol{k}\cdot\boldsymbol{r}(i\cos\theta - \sin\theta)}$$

damp at large r

Eigenvalue problem of complex-scaled Hamiltonian $H(\theta) = U(\theta) H U^{-1}(\theta)$

$$H(\theta)\Psi_\lambda^{JM\pi}(\theta) = E_\lambda(\theta)\Psi_\lambda^{JM\pi}(\theta)$$

can be solved with L^2 basis within suitable $\boldsymbol{\theta}$

$$\Psi_\lambda^{JM\pi}(\theta) = \sum_i C_i^\lambda(\theta)\Phi_i(\boldsymbol{x})$$

$$S(E) = -\frac{1}{\pi} \mathrm{Im} \sum_{\mu} \langle \Psi_0 | \mathcal{M}^{\dagger}_{1\mu} U^{-1}(\theta) R(\theta) U(\theta) \mathcal{M}_{1\mu} | \Psi_0 \rangle$$

$$R(\theta) = \frac{1}{E - H(\theta) + i\epsilon}$$

(complex-scaled resolvent)

$$= -\frac{1}{\pi} \sum_{\mu\lambda} \mathrm{Im} \frac{\widetilde{\mathcal{D}}_\mu^\lambda(\theta)\mathcal{D}_\mu^\lambda(\theta)}{E - E_\lambda(\theta) + i\epsilon}$$

$$\mathcal{D}_\mu^\lambda(\theta) = \left\langle \left(\Psi_\lambda^{JM\pi}(\theta)\right)^* \middle| \mathcal{M}_{1\mu}(\theta) | U(\theta)\Psi_0 \right\rangle$$

The contribution of eigenstate $\boldsymbol{\lambda}$ to S(E) $E_\lambda(\theta) = E_c - \frac{i}{2}\Gamma_c$

$$\frac{1}{\pi}\frac{1}{(E-E_c)^2+\frac{1}{4}\Gamma_c^2}\sum_\mu\left[\frac{1}{2}\Gamma_c \mathrm{Re}\tilde{\mathcal{D}}_\mu^\lambda(\theta)\mathcal{D}_\mu^\lambda(\theta) - (E-E_c)\mathrm{Im}\tilde{\mathcal{D}}_\mu^\lambda(\theta)\mathcal{D}_\mu^\lambda(\theta)\right]$$

Lorentz distribution

θ dependence of H(θ)

kinetic energy $T \to Te^{-2i\theta}$

potential energy

exponential $e^{-r/\mu} \to e^{-r(\cos\theta + i\sin\theta)/\mu}$ $\mu \to \mu/\cos\theta$

Gaussian $e^{-r^2/\mu^2} \longrightarrow e^{-r^2(\cos 2\theta + i\sin 2\theta)/\mu^2}$ $\mu \to \mu/\sqrt{\cos 2\theta}$

$0 < \theta < 45^\circ$

Continuum energy scales as $k^2 e^{-2i\theta}$

Bound states and resonances should be stable against θ

Useful check

Two-body photoabsorption cross section and radiative capture cross section

$\gamma + C \leftrightarrow A + B$

Detailed balance $\sigma_\gamma^{\mathrm{AB}}(E_\gamma) = \dfrac{k^2(2J_A+1)(2J_B+1)}{2k_\gamma^2(2J_0+1)}\sigma_{\mathrm{cap}}^{\mathrm{AB}}(E_{\mathrm{in}})$ $E_{\mathrm{in}} = E_\gamma - E_{\mathrm{th}}$

$\sigma_{\mathrm{cap}}^{\mathrm{AB}}$ can be calculated in a standard reaction theory: serve as a test of CSM

Photoabsorption of ^{4}He

$$\sigma_\gamma(E_\gamma) = \frac{4\pi^2}{\hbar c} E_\gamma \frac{1}{3} S(E_\gamma)$$

Physics motivation:

Experimental discrepancy in low-energy σ_γ

E1 sum rule

Basis functions for E1 excitation:

sum rule, 2- and 3-body decay channels

(cluster model)

$$\Psi_f^{\mathrm{sp}} = \mathcal{A}\big[\Phi_0^{(4)}(i)\mathcal{Y}_1(\boldsymbol{r}_1 - \boldsymbol{x}_4)\big]_{1M}$$ Important for sum rule

$$\Psi_f^{\mathrm{3N+N}} = \mathcal{A}\big[\Phi_{J_3}^{(3)}(i)\exp\big(-a_3 x_3^2\big)[\mathcal{Y}_1(\boldsymbol{x}_3)\chi_{\frac{1}{2}}(4)]_j\big]_{1M}$$

$$\Psi_f^{\mathrm{d+p+n}} = \mathcal{A}\big[\Phi_{J_3}^{(\mathrm{dN})}(i)\exp\big(-a_3 x_3^2\big)[\mathcal{Y}_0(\boldsymbol{x}_3)\chi_{\frac{1}{2}}(4)]_{\frac{1}{2}}\big]_{1M}$$

$$\Phi_{J_3}^{(\mathrm{dN})}(i) = \big[\Psi_{J_2}^{(2)}(i)\exp\big(-a_2 x_2^2\big)[\mathcal{Y}_1(\boldsymbol{x}_2)\chi_{\frac{1}{2}}(3)]_j\big]_{J_3}$$

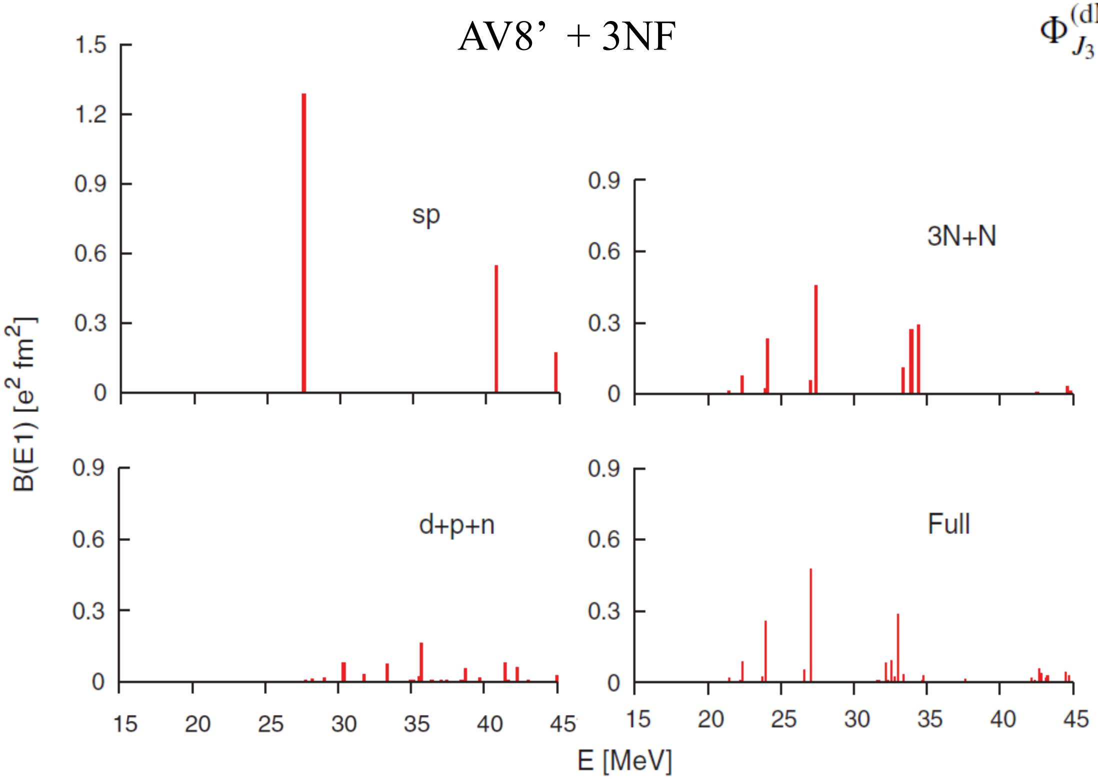

coordinates acted by E1 operator

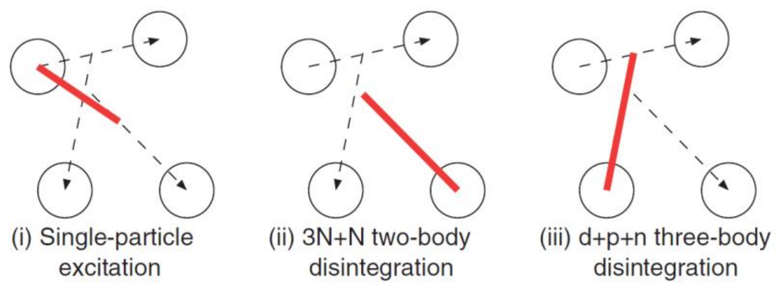

Comparison with experiment

θ dependence

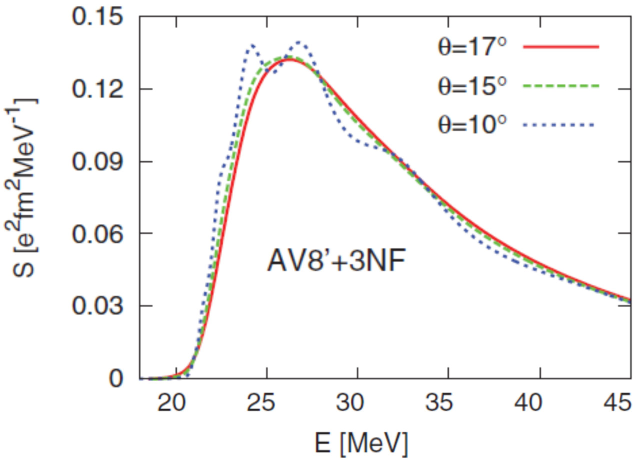

Check of CSM

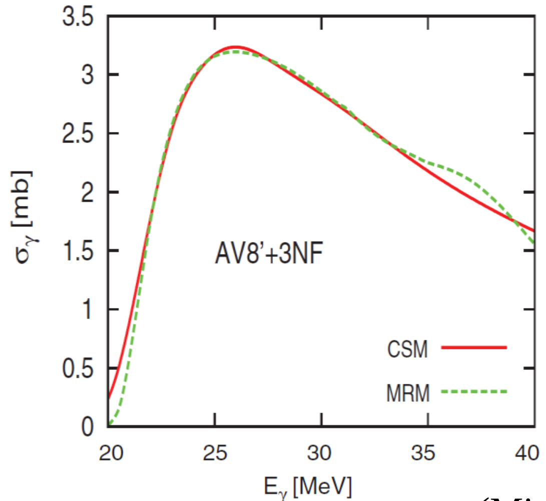

$\sigma_\gamma^{^3\mathrm{H}\,p} + \sigma_\gamma^{^3\mathrm{He}\,n}$

(Microscopic R-matrix calculation)

CSM, θ=17°

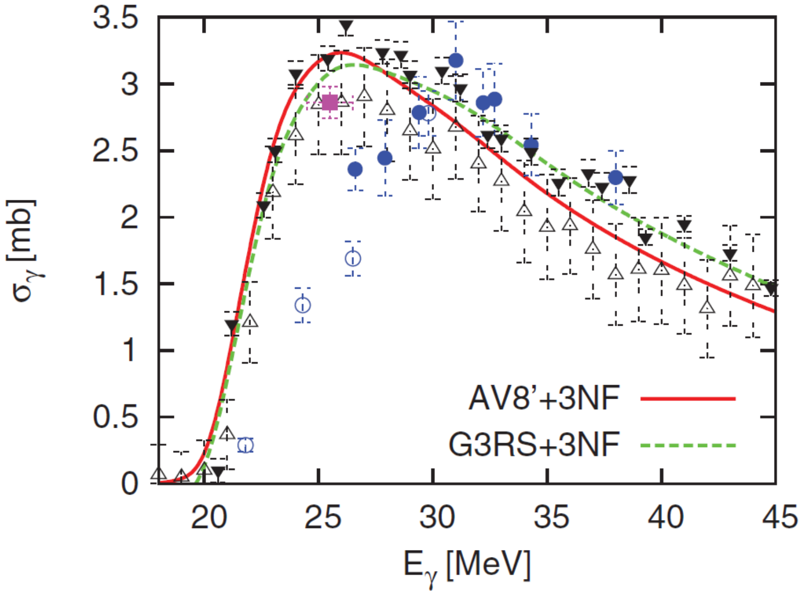

Sum rule

$$m_\kappa(E_{\max}) = \int_0^{E_{\max}} E_\gamma^\kappa \sigma_\gamma(E_\gamma)\, dE_\gamma$$

NEWSR $\quad m_{-1}(\infty) = \mathcal{G}\left(Z^2\langle r_p^2\rangle - \frac{Z(Z-1)}{2}\langle r_{pp}^2\rangle\right)$ $\quad \mathcal{G} = 4\pi^2 e^2/3\hbar c$

Fully satisfied

EWSR $\quad m_0(\infty) = \mathcal{G}\frac{3NZ\hbar^2}{2Am_N}(1+K)$

Enhancement factor $\quad K = \sum_q K_q \qquad V_{2\mathrm{NF}} = \sum_q V_q$

$$K_q = \frac{2Am_N}{3NZ\hbar^2 e^2}\frac{1}{2}\sum_\mu \langle\Psi_0|[\mathcal{M}_{1\mu}^\dagger, [V_q, \mathcal{M}_{1\mu}]]|\Psi_0\rangle$$

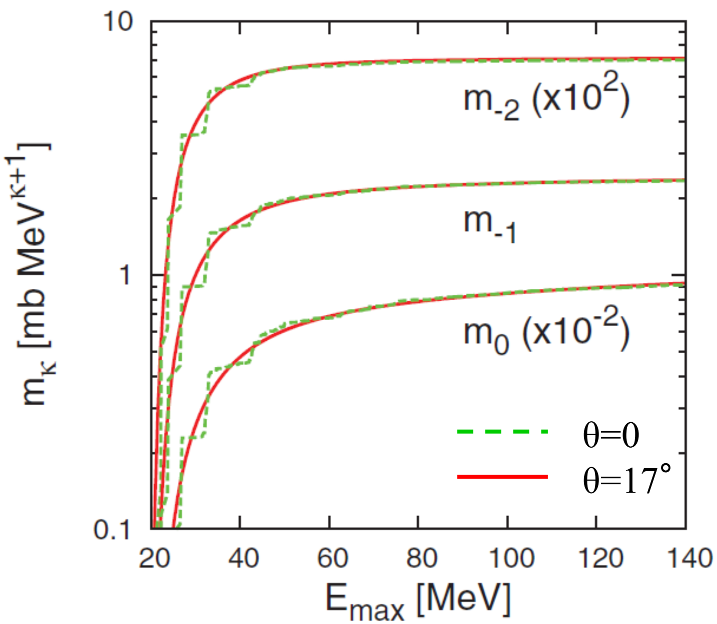

Sum rule by discretized states leads to good correspondence with that of CSM

m_{-2} converges at $m_\pi c^2$, while m_0 occupies 73% of $m_0(\infty)$

q		$\langle V_q\rangle$	K_q
1	1	17.39	0
2	$\boldsymbol{\sigma}_i \cdot \boldsymbol{\sigma}_j$	−9.59	0
3	$\boldsymbol{\tau}_i \cdot \boldsymbol{\tau}_j$	−5.22	0.011
4	$\boldsymbol{\sigma}_i \cdot \boldsymbol{\sigma}_j \boldsymbol{\tau}_i \cdot \boldsymbol{\tau}_j$	−59.42	0.460
		(−12.51)	(0.187)
5	S_{ij}	0.75	0
6	$S_{ij}\boldsymbol{\tau}_i \cdot \boldsymbol{\tau}_j$	−70.93	0.574
		(−68.65)	(0.667)
7	$(\boldsymbol{L}\cdot\boldsymbol{S})_{ij}$	11.09	0
8	$(\boldsymbol{L}\cdot\boldsymbol{S})_{ij}\boldsymbol{\tau}_i \cdot \boldsymbol{\tau}_j$	−15.93	0.061
	Total	−131.9	1.11

Major contribution by one-pion exc. force

Spin-dipole excitations of ^{4}He

SD resonance is narrower than E1 resonance

SD operator $$\sum_{i=1}^{N}[\boldsymbol{\rho}_i \times \boldsymbol{\sigma}_i]_{\lambda\mu} T_i^p$$

$$\boldsymbol{\rho}_i = \boldsymbol{r}_i - \boldsymbol{x}_N$$

$$T_i^p = \begin{cases} 1 & \text{Isoscalar (IS)} \\ \tau_z(i) & \text{Isovector (IV0)} \\ t_{\pm}(i) & \text{Charge-exc.(IV}\pm\text{)} \quad (^4\text{H}, {}^4\text{Li}) \end{cases}$$

λ=0,1,2 (multipolarity)

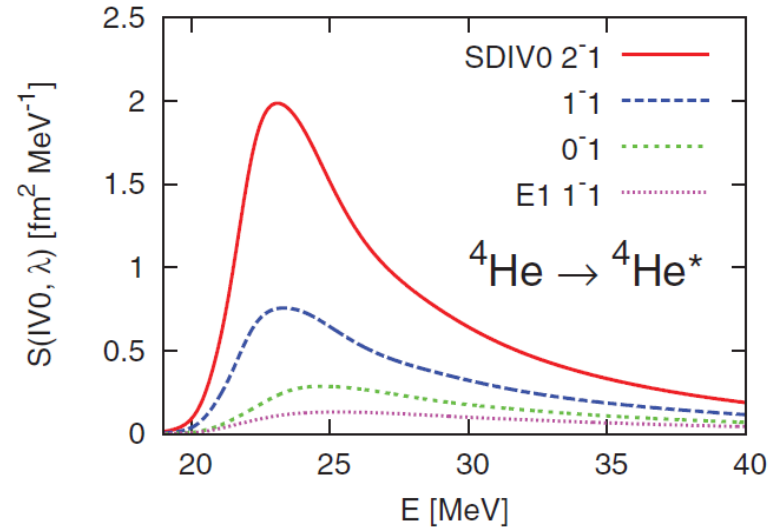

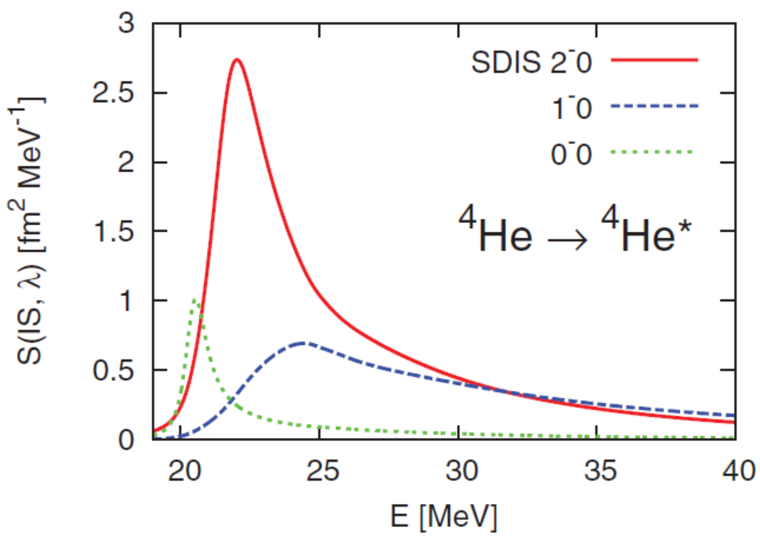

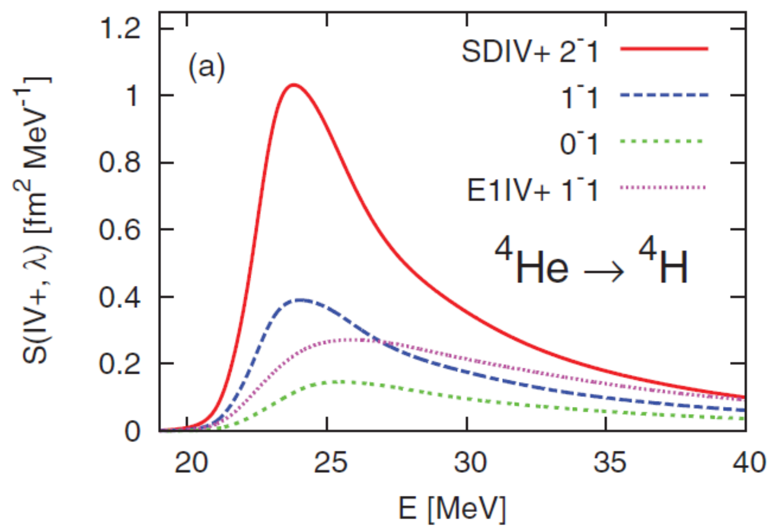

Good correspondence between the peak energy and the resonance energy

Resonance parameters

$J^\pi T$	^{4}He E_R $E(\theta)$	$S(E)$	Exp.	Γ $E(\theta)$	$S(E)$	Exp.
0^-0	20.42	20.54	21.01	0.96	1.06	0.84
2^-0	21.67	22.03	21.84	2.12	3.10	2.01
2^-1	23.63	23.11	23.33	4.99	5.58	5.01
1_1^-1	23.86	23.34	23.64	5.31	7.17	6.20
1^-0	24.32	24.44	24.25	5.40	9.57	6.10
0^-1	25.67	24.71	25.28	7.60	9.98	7.97
1_2^-1		25.36	25.95		13.24	12.66

E(θ): Stable eigenvalues of H(θ)
S(E): Peaks of strength function
B.A.: Bound-state approximation

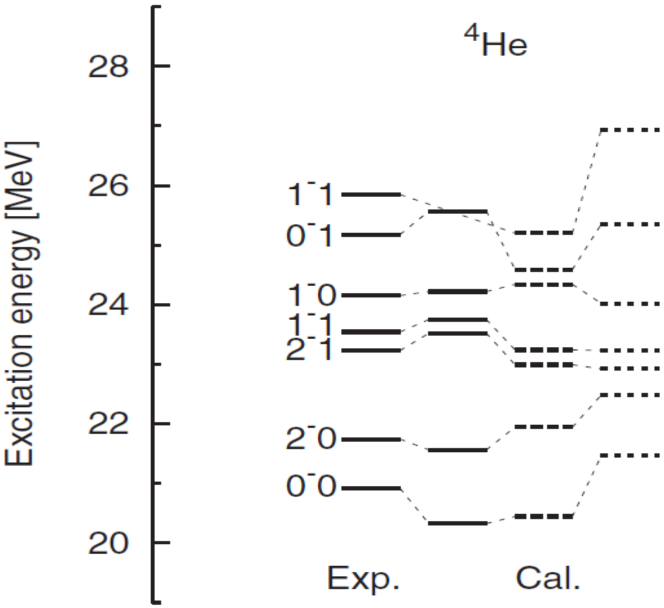

E(θ) S(E) B.A.

Almost no data that can be compared to theoretical SD strength functions

Charge-exc. reaction $^4\text{He}(^7\text{Li},{}^7\text{Be}\gamma)$

Spin-nonflip parts ⟶ E1

Spin-flip parts ⟶ SD

Nakayama et al., PRC76 (2007)

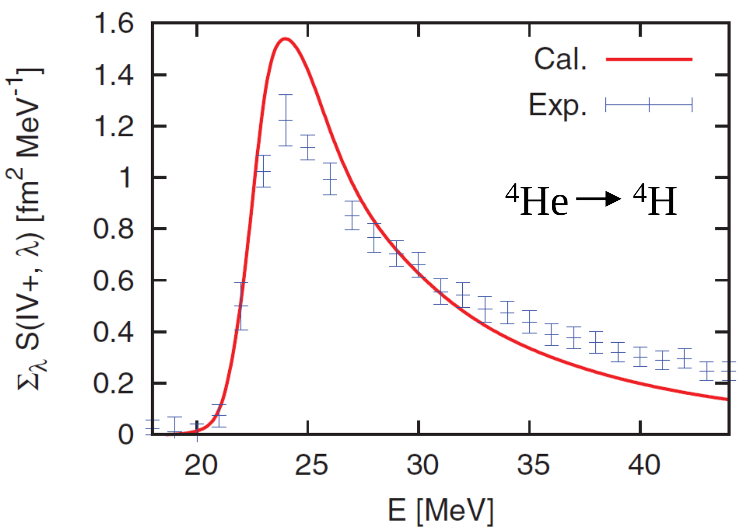

Electric dipole excitations of halo nuclei

^{6}He

α+n+n three-body model is fairly good
E1 response of ^{6}He has so far been studied within the three-body model

E1 strength is calculated in 6-body model that makes it possible
to treat **both low- and high-lying strengths**
Minnesota potential fitted to S_{2n} is used (u=1.05)

^{6}He ground state in six-body model
good convergence in a small dimension

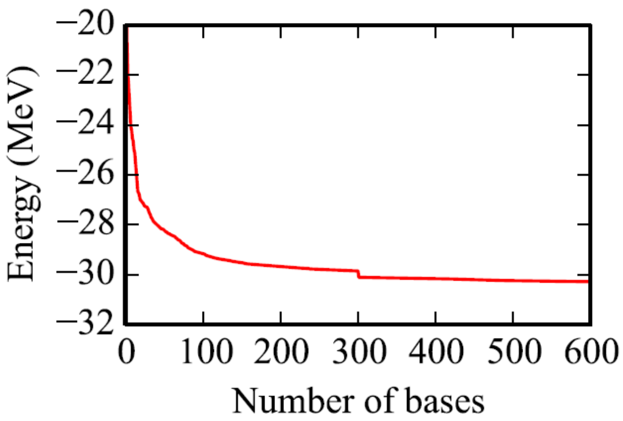

Comparison of B(E1) for ^{4}He

Minnesota

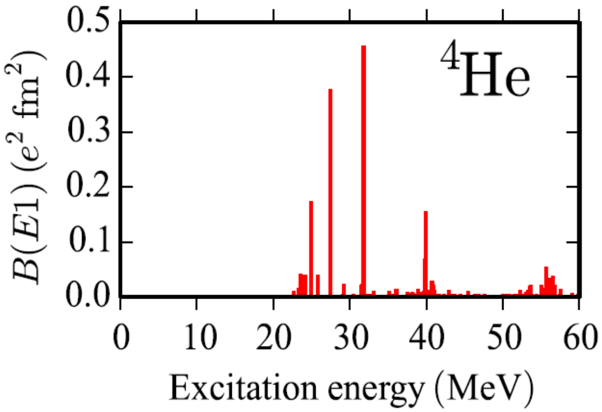

AV8’

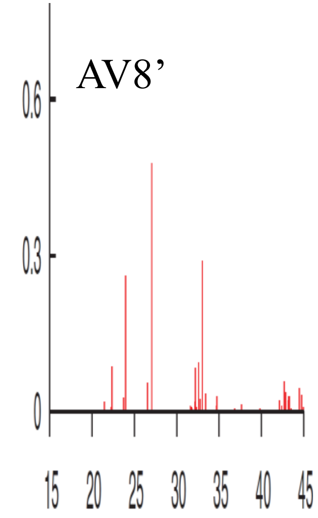

Calculation is continuum discretization taking into account
3-body decay channels of **α**+n+n and t+d+n

Basis dimension used for $J^{\pi}=1^{-}$ (T=1, 2, 3) continuum is about 14,000

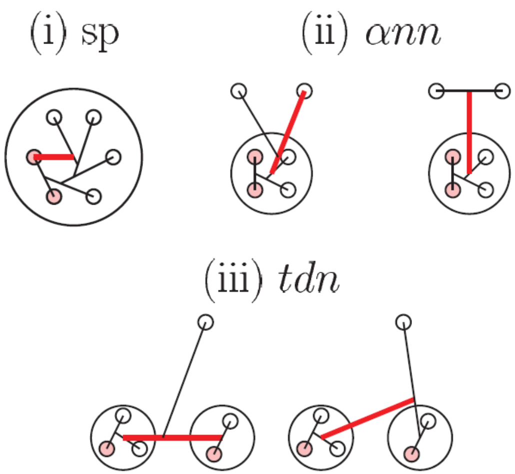

E1 strength

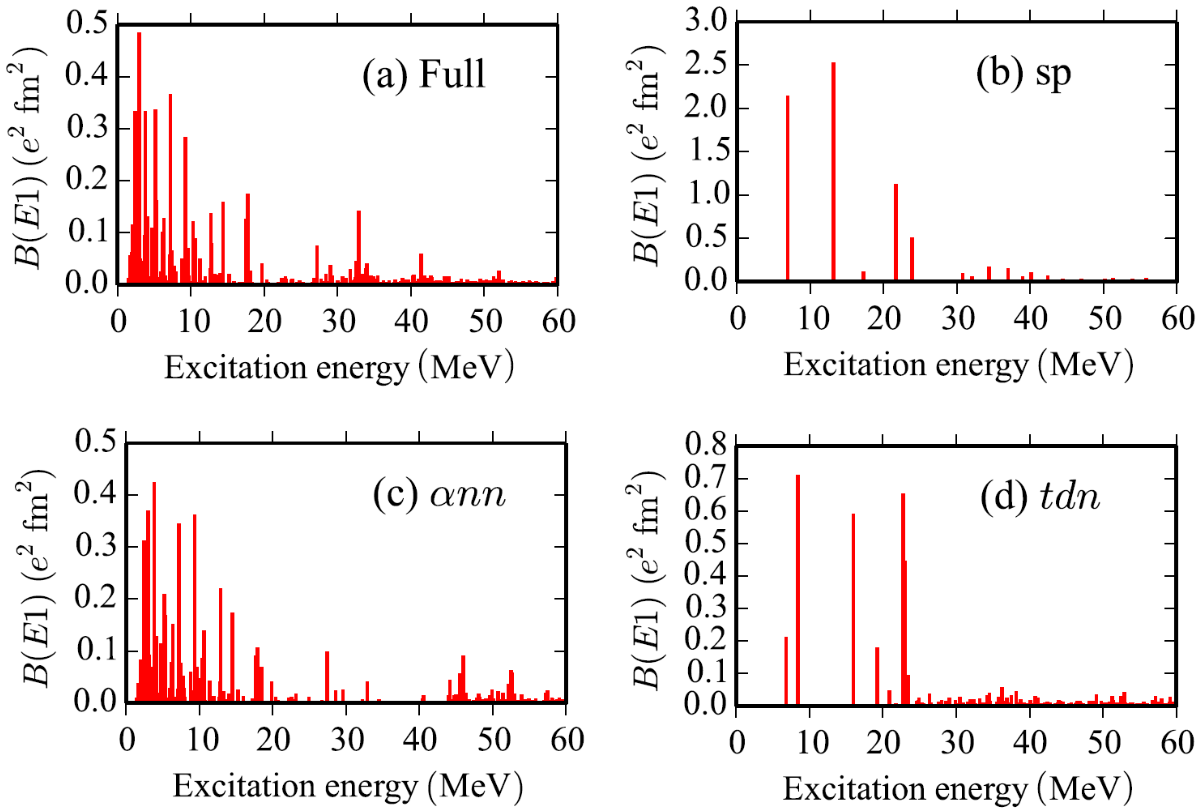

Smearing with Lorenzians

$$\frac{dB(E1,E)}{dE} = \sum_{\nu} N(E_\nu,\Gamma) L(E,E_\nu,\Gamma) B(E1,\nu)$$

$$L(E,E_\nu,\Gamma) = \frac{\Gamma}{2\pi} \frac{1}{(E-E_\nu)^2 + (\Gamma/2)^2}$$

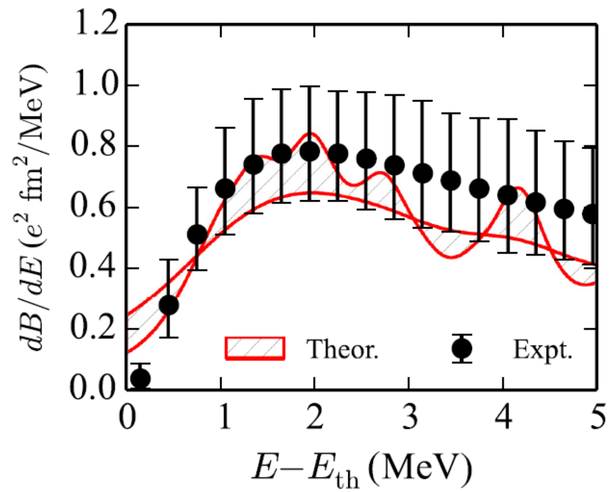

Γ=0.75-2.0 MeV

Aumann et al., PRC59 (1999)

SDM vs GDR

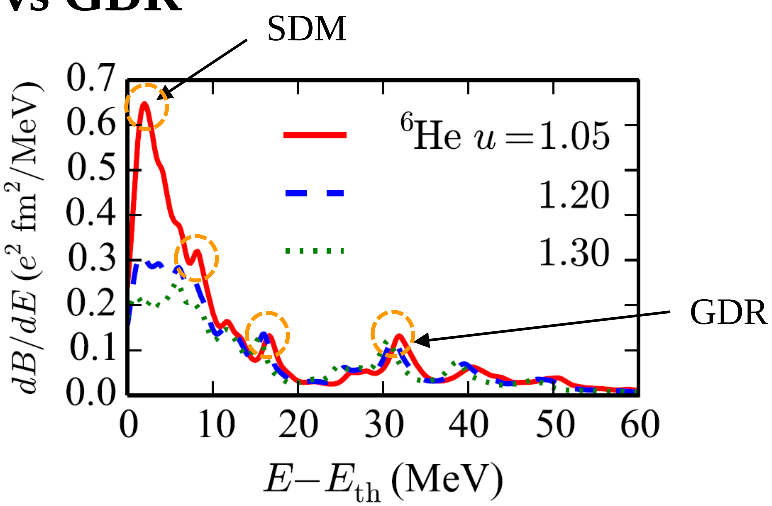

u=1.05 reproducing S_{2n} leads to the enhancement of low-lying strength (SDM)

Larger u leads to stronger binding of neutrons:

SDM shrinks but GDR survives

A few peaks exists between SDM and GDR

SDM peak is much larger than GDR peak

Proton-proton rms distance of the discretized continuum states

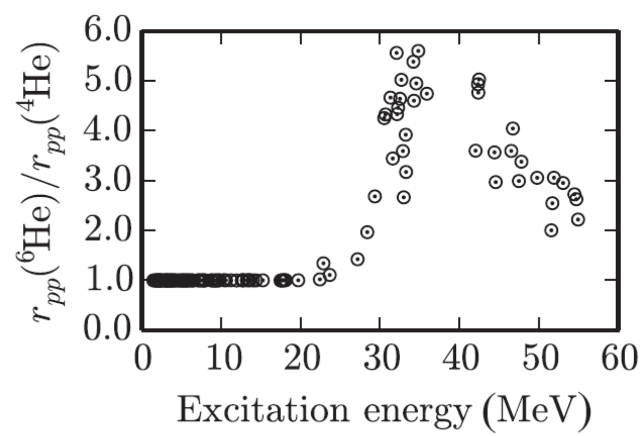

sudden rise at about 25 MeV

Proton and neutron transition densities

$$\rho^{\mathrm{tr}}_{p/n}(E_\nu, r) = \langle \Psi_1(E_\nu) \| \sum_{i \in p/n} \mathcal{Y}_1(\boldsymbol{r}_i - \boldsymbol{x}_6)\, \delta(|\boldsymbol{r}_i - \boldsymbol{x}_6| - r) \| \Psi_0 \rangle$$

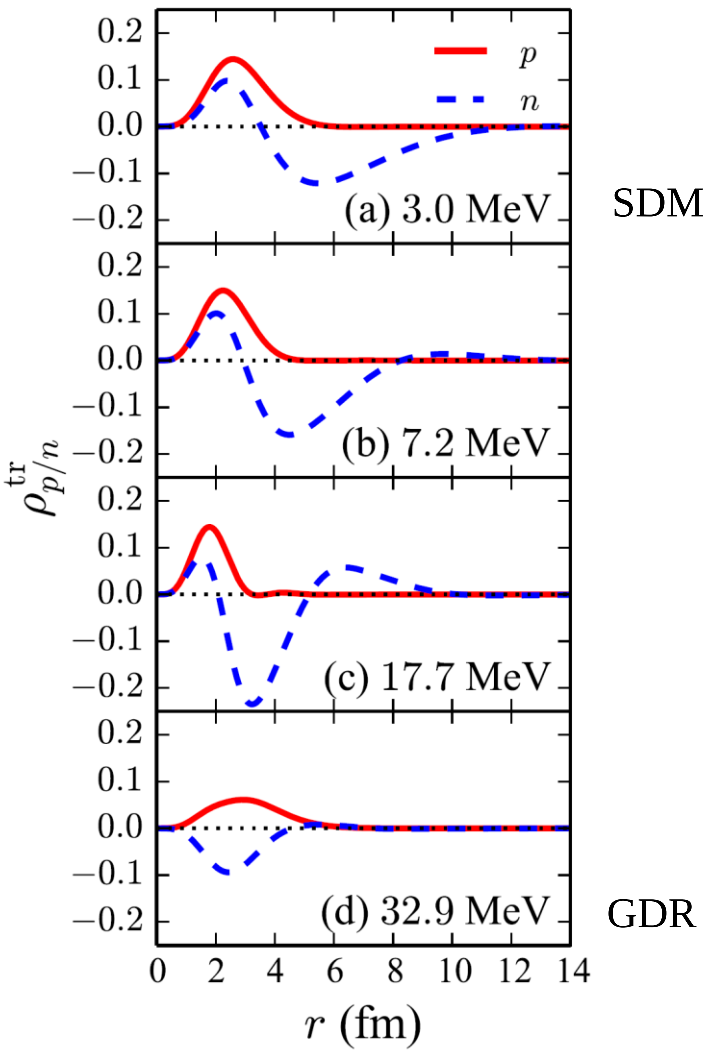

Below 25 MeV:
- In-phase oscillation inside the ^{4}He core
- Out-of-phase oscillation near the surface
- Growing oscillations of halo neutrons with E

Completely out-of-phase at GDR

E1 NEWSR

$$\sum_{\nu} B(E1,\nu) = e^2\left(Z^2\langle r_p^2\rangle - \frac{Z(Z-1)}{2}\langle r_{pp}^2\rangle\right) \qquad 7.21\ e^2\ \mathrm{fm}^2$$

Full model accounts for 99.9% of NEWSR

Cluster sum rule (CSR)

Alhassid, Gai, Bertsch, PRL 49 (1982)

$$B(E1;\mathrm{NEWCSR}) = e^2\left(\frac{2Z}{A}\right)^2\langle \boldsymbol{R}^2\rangle \qquad 5.44\ e^2\ \mathrm{fm}^2$$

(75% of NWESR)

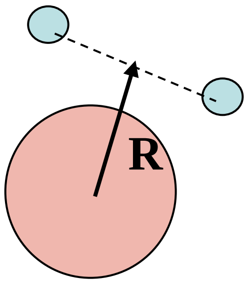

Maximum excitation energy that exhausts CSR

$$\sum_{\nu=1}^{\nu_{\max}} B(E1,\nu) \qquad E_{\nu_{\max}} = 26.8\ \mathrm{MeV}$$

SDM and GDR are well separated

E1 strength below 25 MeV is understood with **α**+n+n 3-body structure

SDM consists of T=1 states while GDR of T=2 states

^{22}C

Neutron-dripline nucleus

Borromean as ^{20}C+n+n system (S-wave 2n halo)

Very large matter radius from reaction cross section; 5.4±0.9 fm

Tanaka et al., PRL104 (2010)

Very small but poorly known S_{2n}; -0.14±0.46 MeV Gaudefroy et al., PRL109 (2012)

The aim is to study both the ground state properties and low-lying E1 strength without assuming the ^{20}C core

Mean-field approach with Skyrme energy density functionals

Random-phase approximation

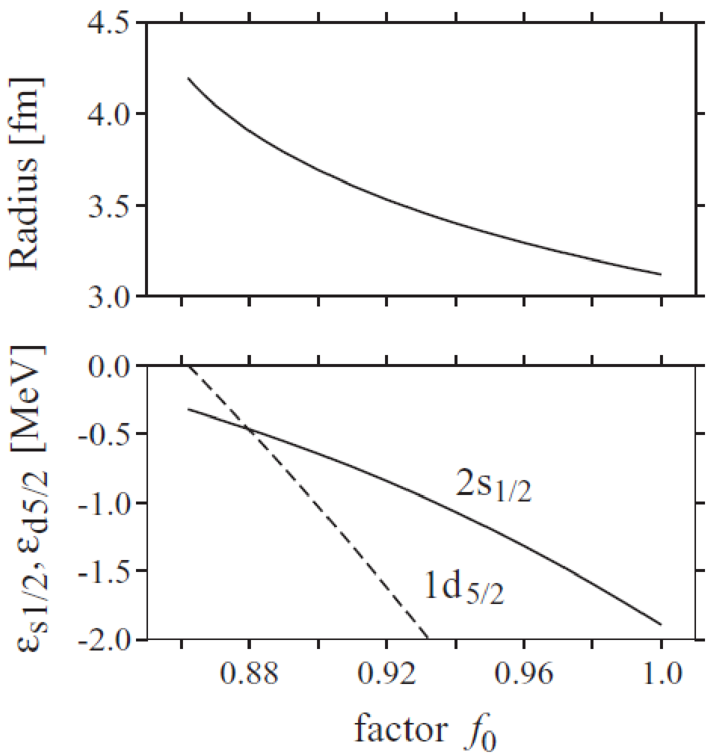

Difficult to reproduce 3-body structure

SIII central part is weakened to reproduce the dripline features

f_0=0.884: ε_F=-0.5 MeV

rms matter radius=3.89 fm

rms radius of $2s_{1/2}$ orbit=7.20 fm

$2s_{1/2}$ and $1d_{5/2}$ orbits are nearly degenerate

(S_{2n} negative: ^{22}C spherical, ^{20}C oblate)

E1 strength

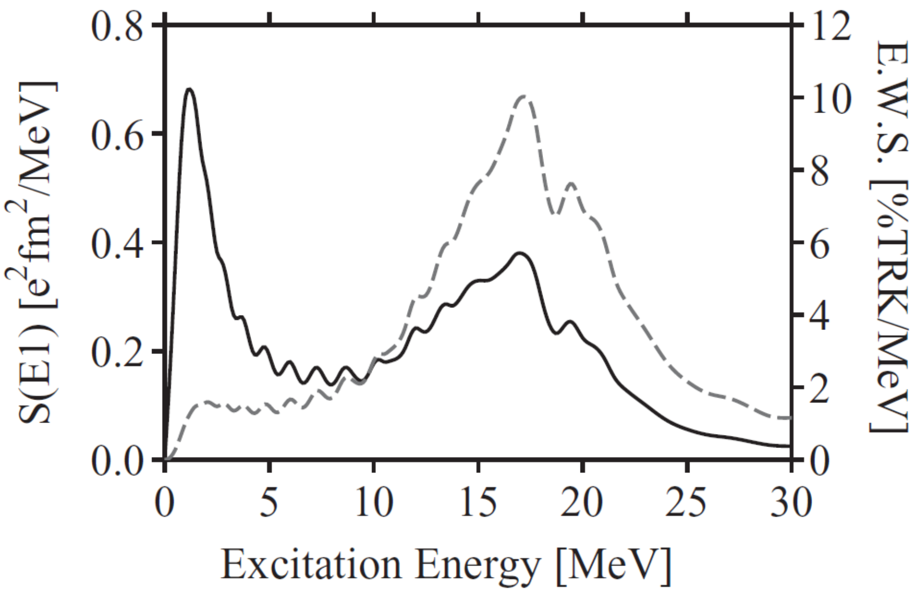

Large low-lying strength comparable
to that of GDR
'Giant' low-lying resonance
(much larger than usual PDR)
EWS occupies 6 and 15 % of TRK sum
at E_{exc}=5 and 10 MeV, respectively
EWS exceeds EWCSR at E_{exc}=3.3 MeV
$1d_{5/2}$ orbit excitation is important

^{20}C+n+n 3-body model

Ershov,Vaagen,Zhukov, PRC86 (2012)

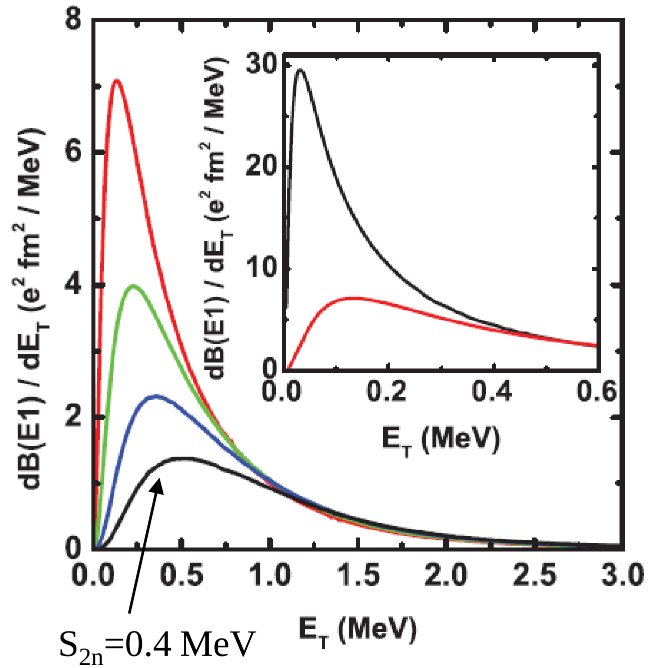

FIG. 6. (Color online) Calculated ^{22}C dipole strength function distributions for separation energies S_{2n} = 50, 100, 200, and 400 keV (upper to lower curves). The insert compares dipole strength distributions for S_{2n} = 10 keV (upper line) and 50 keV (lower line).

Low-lying strength is very sensitive to S_{2n}
The effect of core excitation makes
difference beyond E_{exc} > 2MeV

E1 transition density

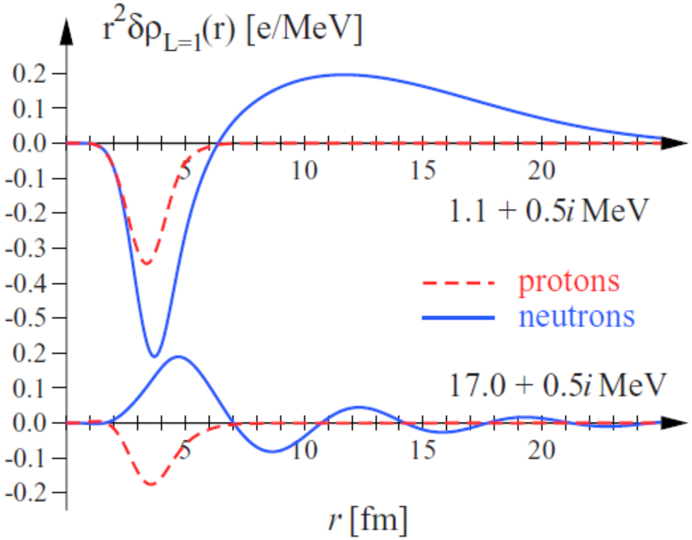

Neutron transition density decomposed into occupied orbits

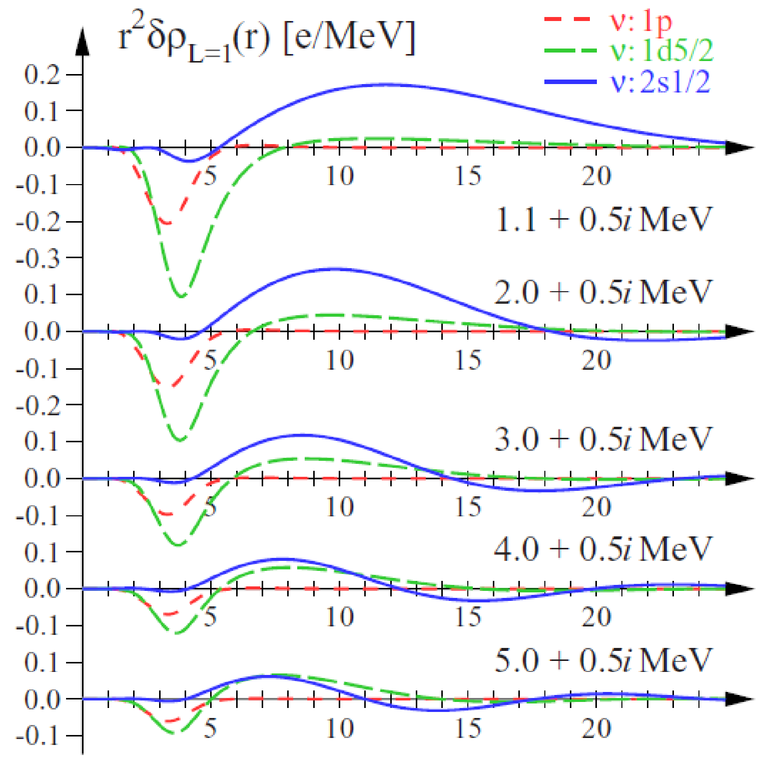

GDR peak: out-of-phase inner oscillation
  with oscillating extended neutron tail
Low-lying peaks: SDM like pattern
  Neutron density extends to 25 fm

Comparison of E1 strength between ^{6}He and ^{22}C

The pattern of the strength is similar, but the origin of the strength between low-lying resonance and GDR is not the same:

- halo-neutron excitation in ^{6}He
- both halo-neutron and $1d_{5/2}$ orbit excitations in ^{22}C
- (may depend on the degeneracy of orbits near Fermi surface)

^{12}C+n+n+p+p calculation for 0^+ states in ^{16}O

^{16}O is doubly magic
The first excited state is 0^+ at 6.05 MeV
Contradiction to the shell-model filling of single particle orbits
Multiparticle-multihole (esp. 4p-4h) configurations in deformation
Shape coexistence

Several recent attempts:
Configuration mixing of Slater determinants — Bender,Heenen NPA713 (2003)
Shinohara et al., PRC74 (2006)
Large-scale calculations: NCSM — Maris et al., PRC79 (2009)
CCT — Wloch et al., PRL94 (2005)

Semi-microscopic ^{12}C+**α** 2-cluster model — Suzuki, PTP55,56 (1976)
Rotation of ^{12}C and Pauli constraint for two-cluster relative motion
All T=0 levels below E_{exc}=15 MeV but 10.96(0^-) are reproduced
Electric transitions and α-decay widths

The aim is to understand the coexisting mechanism by performing 5-body calculation without assuming a preformed α-cluster
^{12}C is assumed to remain in its ground state
4-nucleon dynamics is solved by excluding the occupied orbits in ^{12}C

$$H = T_v + T_{cv} + V_v + V_{cv}$$

$T_v = \sum_{i=1}^{4} T_i - T_{\mathrm{c.m.}}$ Intrinsic kinetic energy of four valence nucleons

T_{cv} Kinetic energy between c-v

$V_v = \sum_{i<j} v_{ij}$ Potential energy among valence nucleons

$V_{cv} = \sum_{i=1}^{4} U_i$ Potential energy between c-v

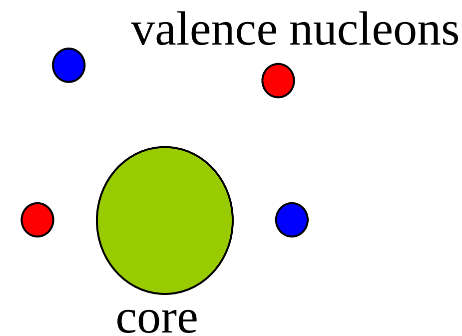

Minnesota potential, Woods-Saxon potential to fit ^{13}C ($1/2^-$, $1/2^+$, $5/2^+$)

Pauli constraint: $\Gamma_i |\Psi\rangle = 0$ Projection operator onto $0s_{1/2}$ and $0p_{3/2}$ HO orbits

Add a pseudo potential $\lambda \sum_{i=1}^{4} \Gamma_i$ to Hamiltonian

λ is taken very large

Basis functions

$$\mathcal{A}\left\{e^{-\frac{1}{2}\tilde{x}Ax}\left[\left[\mathcal{Y}_{L_1}(\tilde{u}_1 \boldsymbol{x})\mathcal{Y}_{L_2}(\tilde{u}_2 \boldsymbol{x})\right]_L \chi_L\right]_{00}\eta_{TM_T}\right\}$$

L=0,1,2; T=0

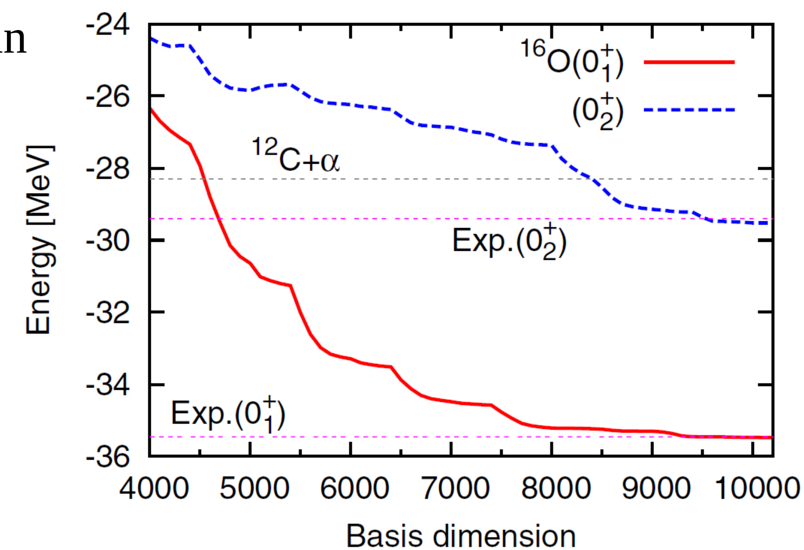

Calculation reproduces the two 0^+ states in agreement with experiment

Slow convergence because many bases are needed to eliminate the forbidden states

Properties of the two 0^+ states

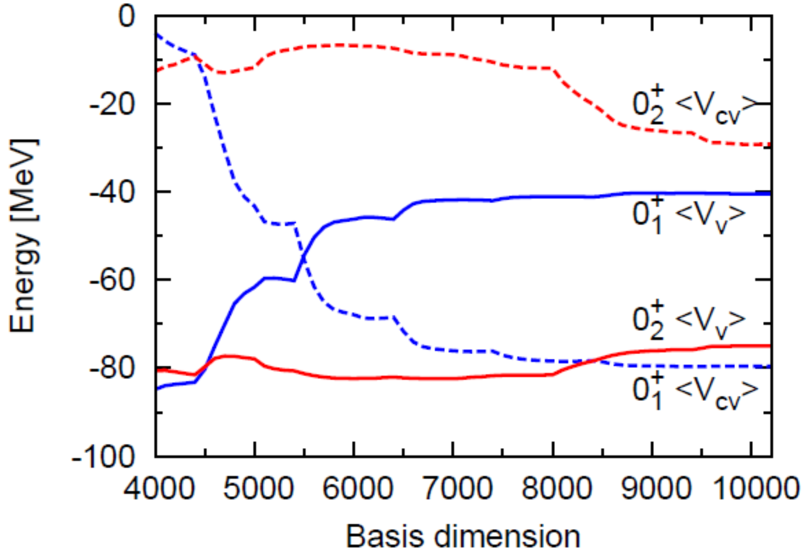

	^{16}O (0_1^+)	^{16}O (0_2^+)	α
E	-35.47	-29.52	-28.30
$E_{\text{expt.}}$	-35.46	-29.41	-28.30
$\langle T_{cv}\rangle$	11.55	7.16	–
$\langle V_{cv}\rangle$	-79.55	-29.22	–
$\langle T_v\rangle$	72.93	67.46	56.92
$\langle V_v\rangle$	-40.41	-74.92	-85.22
$\sqrt{\langle r^2\rangle}$	2.47	3.03	1.43
$\sqrt{\langle r^2\rangle_{\text{expt.}}}$	2.57(2)	–	1.46(1)
$\sqrt{\langle r_{cv}^2\rangle}$	2.54	4.86	–
$\sqrt{\langle r_v^2\rangle}$	1.90	1.62	1.43

Energy contents of four nucleons in the 0_2^+ state are similar to that of **α**-particle

^{12}C+**α** spectroscopic amplitude

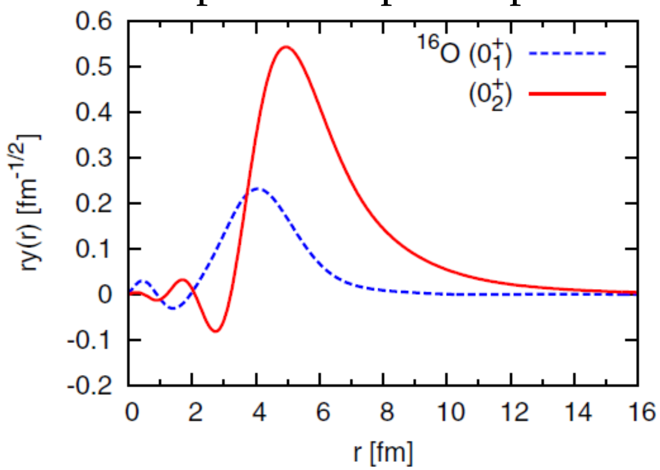

Distribution of HO quanta

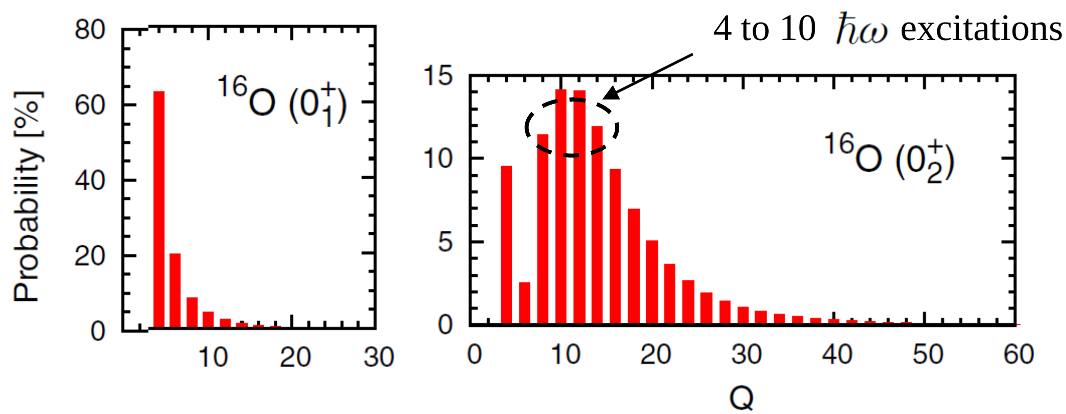

High HO quanta are needed to describe cluster state

Summary

We have applied ECG to bound and continuum problems

Two 0^+ states in both ^{4}He and ^{16}O

Photoabsorption cross section of ^{4}He with CSM

(cluster concept is useful to construct basis functions for decay channels)

E1 response of ^{6}He

Resonances of A=4 systems analyzed with help of response functions

The pseudopotential for eliminating Pauli-forbidden orbits makes convergence very slow: other way to accelerate convergence is desired

Future challenges

Non-inert core plus 4-nucleon approach

^{12}C(0^+, 2^+)+n+n+p+p

1^- states (7.12, 9.58) and 2^+ (6.92) state

E1 and E2 radiative capture reactions ^{12}C(α, γ)^{16}O at Helium burning stage

Isospin impurity has to be taken into account for E1

^{208}Pb(0^+, 3^-)+n+n+p+p

α-decay width and enhanced E1 transitions in ^{212}Po

Varga, Lovas, Liotta, PRL 69 (1992); NPA 550 (1992)

Astier et al., PRL 104 (2010)

Collaborators and References:

ECG with realistic forces:

Y.S., W. Horiuchi, M. Orabi, K. Arai, FBS 42 (2008)

S. Aoyama, K. Arai, Y.S., P. Descouvemont, D. Baye, FBS 52 (2012)

^{4}He:

W. Horiuchi, Y.S., PRC 78 (2008), PRC 87 (2013), FBS 54 (2013), PRC 90 (2014)

W. Horiuchi, Y.S., K. Arai, PRC 85 (2012)

^{6}He:

D. Mikami, W. Horiuchi, Y.S., PRC 89 (2014)

^{16}O:

W. Horiuchi, Y.S., PRC 89 (2014)

^{22}C:

T. Inakura, W. Horiuchi, Y.S., T. Nakatsukasa, PRC 89 (2014)

Enhanced E1 transitions in ^{212}Po

$^{208}Pb(^{18}O,\ ^{14}C)$

Astier et al. (2010)

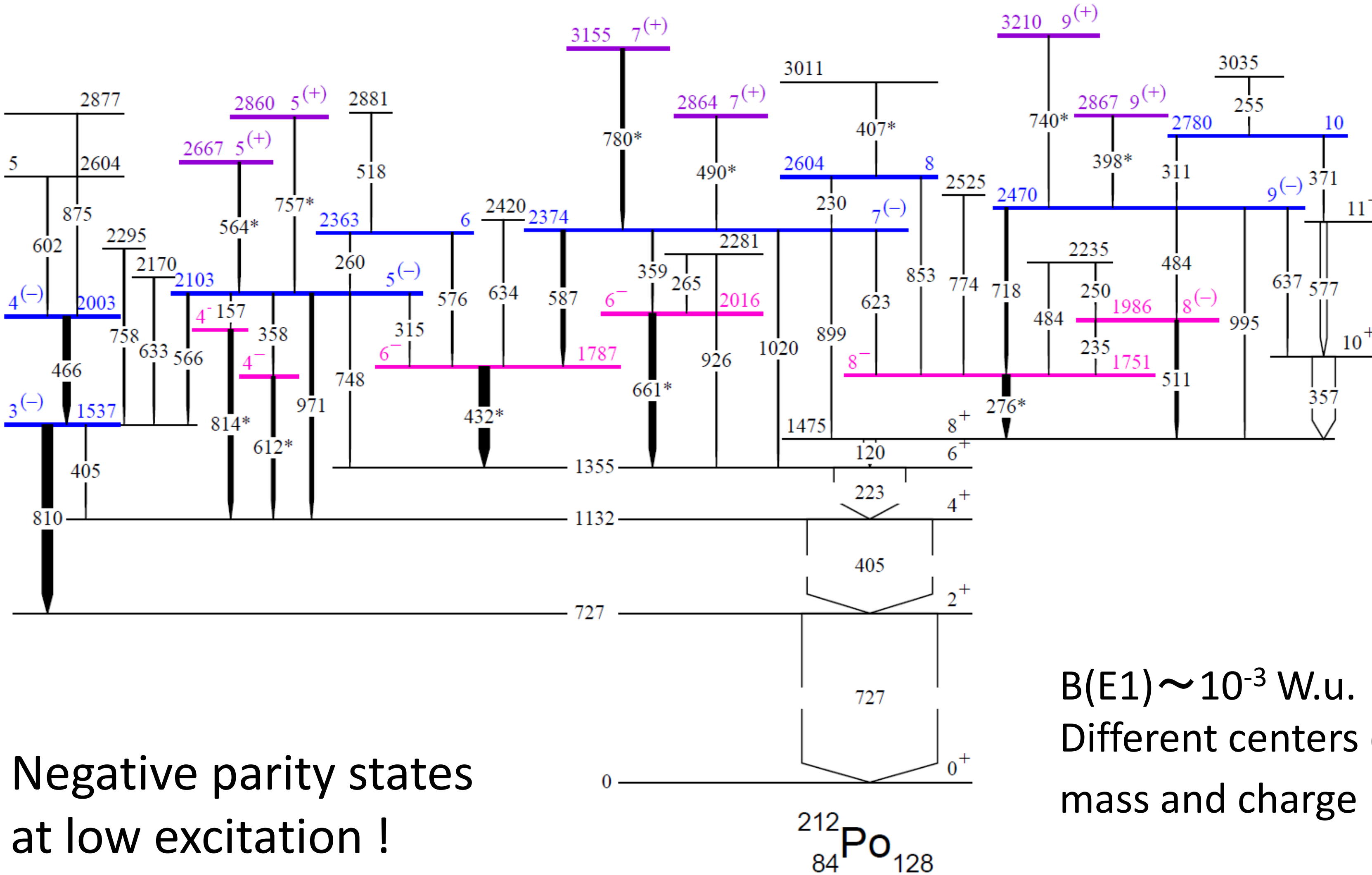

B(E1)～10^{-3} W.u.

Different centers of mass and charge

Negative parity states at low excitation !